MCB
Journals.ASM.org

C1q/Tumor Necrosis Factor-Related Protein 9 Protects against Acute Myocardial Injury through an Adiponectin Receptor I-AMPK-Dependent Mechanism

Takahiro Kambara,[a] Rei Shibata,[a] Koji Ohashi,[b] Kazuhiro Matsuo,[a] Mizuho Hiramatsu-Ito,[a] Takashi Enomoto,[a] Daisuke Yuasa,[a] Masanori Ito,[a] Satoko Hayakawa,[a] Hayato Ogawa,[a] Tamar Aprahamian,[d] Kenneth Walsh,[c] Toyoaki Murohara,[a] Noriyuki Ouchi[b]

Department of Cardiology, Nagoya University Graduate School of Medicine, Nagoya, Japan[a]; Molecular Cardiovascular Medicine, Nagoya University Graduate School of Medicine, Nagoya, Japan[b]; Molecular Cardiology/Whitaker Cardiovascular Institute, Boston University School of Medicine, Boston, Massachusetts, USA[c]; Renal Section, Department of Medicine, Boston University School of Medicine, Boston, Massachusetts, USA[d]

Obesity is a risk factor for cardiovascular disease. C1q/tumor necrosis factor-related protein 9 (CTRP9) is an adipokine that is downregulated by obesity. We investigated the role of CTRP9 in cardiac injury with loss-of-function genetic manipulations and defined the receptor-mediated signaling pathway downstream of this adipokine. CTRP9-knockout (CTRP9-KO) mice at the age of 12 weeks were indistinguishable from wild-type (WT) mice under basal conditions. CTRP9-KO mice had exacerbated contractile left ventricle dysfunction following intraperitoneal injection of lipopolysaccharide (LPS) compared to WT mice. Administration of LPS to CTRP9-KO mice also resulted in increased expression of proinflammatory cytokines and oxidative stress markers in the heart compared to WT mice. Likewise, CTRP9-KO mice showed increased myocardial infarct size and elevated expression of inflammatory mediators in ischemic heart following ischemia and reperfusion compared to WT mice. Treatment of cardiac myocytes with CTRP9 protein led to suppression of LPS-induced expression of proinflammatory genes, which was reversed by blockade of AMPK or ablation of adiponectin receptor I (AdipoR1). Systemic delivery of CTRP9 attenuated LPS-induced cardiac dysfunction in WT mice but not in muscle-specific transgenic mice expressing dominant-negative mutant form of AMPK or in AdipoR1-knockout mice. CTRP9 protects against acute cardiac damage in response to pathological stimuli by suppressing inflammatory reactions through AdipoR1/AMPK-dependent mechanisms.

Obesity causes the progression of various cardiovascular disorders, including ischemic heart disease (1, 2). Adipose tissue functions as an endocrine organ by producing various bioactive secreted proteins, also known as adipokines, that can directly affect the nearby or remote tissues (3). Most adipokines promote obese complications with proinflammatory properties. In contrast, a few numbers of adipokines such as adiponectin are downregulated in obese states, and these factors typically exert salutary actions on obesity-linked cardiovascular disorders (3, 4).

C1q/tumor necrosis factor-related protein families (CTRPs) are conserved paralogs of adiponectin that contain collagen-like and globular C1q-like domains (5). CTRP9 has the highest amino acid identity to adiponectin among CTRPs (6). Like adiponectin, CTRP9 is abundantly expressed in adipose tissue. Plasma CTRP9 levels are reduced in diet-induced or leptin-deficient obese mice (6). Clinically, CTRP9 levels associate negatively with visceral fat adiposity and positively with favorable glucose or metabolic phenotypes (7).

Several experimental studies demonstrated that CTRP9 acts as an adipokine that modulates metabolic and cardiovascular function. Systemic delivery of CTRP9 lowers glucose levels in obese mice (6). Transgenic overexpression of CTRP9 is protective against diet-induced obesity and glucose intolerance (8), whereas CTRP9-deficiency exacerbates insulin resistance and hepatic steatosis (9). These results suggest that CTRP9 plays a physiological role in glucose homeostasis. It has also been shown that CTRP9 promotes endothelium-dependent vasorelaxation (10). We have demonstrated that CTRP9 administration attenuates the neointimal hyperplasia in response to vascular injury in wild-type (WT) mice (11). The systemic administration of CTRP9 to WT mice results in reduced myocardial infarct size after the animals were subjected to ischemia and reperfusion (ischemia-reperfusion) (12), and it has been shown that delivery of CTRP9 protein improves cardiac function in WT mice after myocardial infarction (13).

Although the overexpression of CTRP9 appears to be effective for attenuating cardiovascular damage and dysfunction, nothing is known about the role of endogenous CTRP9 in cardiovascular diseases. Furthermore, little is known about the molecular mechanism by which CTRP9 modulates cardiac injury *in vivo*. In the present study, we investigated the effect of CTRP9 in two mouse models of cardiac injury using both loss-of-function and gain-of-function genetic manipulations.

Received 25 December 2014 **Returned for modification** 3 February 2015
Accepted 3 April 2015

Accepted manuscript posted online 13 April 2015

Citation Kambara T, Shibata R. Ohashi K, Matsuo K, Hiramatsu-Ito M, Enomoto T, Yuasa D, Ito M, Hayakawa S, Ogawa H, Aprahamian T, Walsh K, Murohara T, Ouchi N. 2015. C1q/tumor necrosis factor-related protein 9 protects against acute myocardial injury through an adiponectin receptor I-AMPK-dependent mechanism. Mol Cell Biol 35:2173–2185. doi:10.1128/MCB.01518-14.

Address correspondence to Rei Shibata, rshibata@med.nagoya-u.ac.jp, or Noriyuki Ouchi, nouchi@med.nagoya-u.ac.jp.

doi:10.1128/MCB.01518-14

MATERIALS AND METHODS

Materials. Antibodies to phospho-AMPK (Thr-172), AMPK, acetyl coenzyme A carboxylase (ACC), phospho-NF-κB (Ser536), and α-tubulin were purchased from Cell Signaling Technology (Massachusetts). Phospho-ACC (Ser-79) antibody was purchased from Upstate Biotechnology. Recombinant human CTRP9 protein and mouse CTRP9 antibody were purchased from Aviscera Bioscience (California). Lipopolysaccharide (LPS), compound C, and SQ22536 were purchased from EMD Millipore (Massachusetts). A mouse tumor necrosis factor alpha (TNF-α) enzyme-linked immunosorbent assay (ELISA) kit was purchased from R&D Systems (Minnesota). Adenoviral vectors containing the gene for β-galactosidase (Ad-β-gal), full-length mouse CTRP9 (Ad-CTRP9) and c-myc-tagged dominant-negative mutant of AMPK (Ad-dn-AMPK) were prepared as described previously (12, 14, 15).

Animals. Male CTRP9 knockout (CTRP9-KO) mice, muscle-specific transgenic mice expressing dominant-negative mutant form of AMPK (dnAMPK-TG) (16), and homozygous adiponectin receptor I knockout (AdipoR1-KO) mice on a C57BL/6J background at 10 to 12 weeks of age were used in the present study. Littermate WT mice were used as controls. The dnAMPK-TG mice were generated by Morris J. Birnbaum's laboratory (University of Pennsylvania). AdipoR1-KO mice were obtained from the MMRC. The study protocols were approved by the Institutional Animal Care and Use Committee of Nagoya University School of Medicine.

CTRP9-KO mice. The CTRP9-KO mouse strain was created from embryonic stem cell clone (C1qtnf9_AE11), generated by Regeneron Pharmaceuticals, Inc. (Tarrytown, NY), the KOMP Repository (www.komp.org), and the Mouse Biology Program (www.mousebiology.org) at the University of California Davis (17). Genotyping primers for the *Ctrp9* WT allele were as follows: 5′-CCTGCACACCAAGGACAGTTAC-3′ (forward) and 5′-TGTCACCTGCATCCACACTTC-3′ (reverse). Primers for the *Ctrp9*-null allele were as follows: 5′-GGTAAACTGGCTCGGATTAGGG-3′ (forward) and 5′-TTGACTGTAGCGGCTGATGTTG-3′ (reverse). CTRP9-KO mice were generated in a background of C57BL/6. Homozygous CTRP9-KO and littermate WT mice were used in the present study.

Endotoxin-induced acute cardiac injury model. Mice were intraperitoneally injected with a single dose of lipopolysaccharide (LPS; 10 mg/kg) or phosphate-buffered saline (PBS) as described previously (18). In some experiments, 3×10^8 PFU of Ad-CTRP9 or Ad-β-gal were systemically injected into the tail vein of mice 5 days before LPS injection. In other experiments, the NF-κB inhibitor, pyrrolidine dithiocarbamate (PDTC; 100 mg/kg, Abcam) or vehicle was given by intraperitoneal injection in mice 1 h before LPS treatment.

Mouse model of ischemia reperfusion injury. We subjected mice to myocardial ischemia reperfusion as previously described (12, 19). Briefly, after anesthetization (pentobarbital at 50 mg/kg, given intraperitoneally) and intubation, the left anterior descending (LAD) artery was ligated for 60 min with a suture using a snare occluder and then loosed. At 24 h after reperfusion, the suture was retied, and Evans blue was systemically injected into mice to determine the nonischemic tissue. The heart was excised, cut, and incubated with 2,3,5-triphenyltetrazolium chloride (TTC) to determine the infarcted region. The left ventricular (LV) area, the area at risk (AAR), and the infarct area (IA) were assessed by computerized planimetry using ImageJ.

Echocardiographic analysis. Mice were subjected to transthoracic echocardiography to evaluate cardiac structure and function in the conscious state 6 h after LPS injection (18). Echocardiogram analysis was performed to measure left ventricular (LV) systolic function, the chamber dimensions, and the ratio of the peak velocity of early to late filling of mitral inflow (E/A ratio) using an Acuson Sequoia C-256 machine with a 15-MHz probe. We quantified the LV end systolic diameter, the LV end diastolic diameter, and the %LV fractional shortening (%FS) from M-mode images. The E/A ratio in mice was quantified based on Doppler imaging.

Cell culture. Primary cultures of the neonatal rat ventricular myocytes (NRVMs) were prepared as described previously (12, 19). Isolated myocytes were cultured in Dulbecco modified Eagle medium (DMEM) containing 10% fetal calf serum. Before each experiment, cells were placed in serum-free DMEM for 12 h. For the CTRP9 stimulation studies, cells were pretreated for 4 h in the presence or absence of recombinant CTRP9 protein (10 μg/ml) and subjected to LPS (100 ng/ml) for 6 h. Cells were infected with Ad-β-gal and Ad-dn-AMPK at a multiplicity of infection (MOI) of 10 for 24 h before treatments. In other experiments, the cells were preincubated with compound C (10 μmol/liter), SQ22536 (10 μmol/liter), or vehicle (DMSO) for 60 min before CTRP9 treatment.

For gene ablation studies, NRVMs were transfected with small interfering RNAs (siRNAs) targeting AdipoR1, AdipoR2, or unrelated siRNAs (Dharmacon, Inc., Lafayette, CO) by Lipofectamine 2000 reagent (Invitrogen/Life Technologies, Grand Island, NY) according to the manufacturer's protocol (12). At 24 h after transfection, NRVMs were incubated with recombinant CTRP9 protein.

Measurement of mRNA. Total RNA from cultured cells was prepared by using an RNeasy Micro kit (Qiagen, Valencia, CA) and from heart tissues using an RNeasy lipid tissue minikit (Qiagen) according to the manufacturer's protocols. cDNA from 500 ng of total RNA was synthesized by reverse transcription using ReverTra Ace qPCR RT master mix (Toyobo Life Science, Osaka, Japan) according to the manufacturer's instructions. Quantitative real-time RT-PCR analysis was performed on a CFX-96 system using Thunderbird qPCR mix (Toyobo Life Science) as a double-stranded DNA-specific dye according to the manufacturer's instructions (Bio-Rad, Hercules, CA) (20). Primers were designed as follows: 5′-ACCACCATCAAGGACTC-3′ and 5′-TGACCACTCTCCCTTTG-3′ for mouse TNF-α, 5′-TTCCAATGCTCTCCTAACAG-3′ and 5′-CTAGGTTTGCCGAGTAGATC-3′ for mouse interleukin-6 (IL-6), 5′-AAACGGTTTGTCTTCAAC-3′ and 5′-ATGGTGAAGTCAATTATGTC-3′ for mouse IL-1β, 5′-CCACTCACCTGCTGCTACTCAT-3′ and 5′-TGGTGATCCTCTTGTAGCTCTCC-3′ for mouse MCP-1, 5′-TCCTTCTTGGGTATGGAATC-3′ and 5′-TAGAGGTCTTTACGGATGTC-3′ for mouse β-actin, 5′-TTGGGTCAGCACTGGCTCTG-3′ and 5′-TGGCGGTGTGCAGTGCTATC-3′ for mouse $gp91^{phox}$, 5′-CTGGCTGAGGCCATCAGACT-3′ and 5′-AGGCCACTGCAGAGTGCTTG-3′ for mouse $p67^{phox}$, 5′-GATGTTCCCCATTGAGGCCG-3′ and 5′-GTTTCAGGTCATCAGGCCGC-3′ for mouse $p47^{phox}$, 5′-TGGTGAACGTGGTGCCTACA-3′ and 5′-TGCAGTCACATCCCACCCT-3′ for mouse CTRP9, 5′-CCAATCTGTGTCCTTCTAAC-3′ and 5′-GTTTCTGAGCATCGTAGTTG-3′ for rat TNF-α, 5′-AAGGTCACTATGAGGTCTAC-3′ and 5′-CATATTGCCAGTTCTTCGTA-3′ for rat IL-6, and 5′-GGTCATCACTATCGGCAATG-3′ and 5′-AGGTCTTTACGGATGTCAAC-3′ for rat β-actin. The expression levels of examined transcripts were compared to that of β-actin and normalized to the mean value of controls.

Western blot analysis. Heart tissue and cell samples were prepared in lysis buffer containing 1 mM phenylmethylsulfonyl fluoride (Sigma). The protein concentration was calculated using a BCA protein assay kit (Thermo Scientific). Equal amounts of proteins were separated by denaturing SDS-PAGE. Proteins were transferred onto polyvinylidene difluoride membrane (Bio-Rad) and probed with the primary antibody, followed by incubation with the horseradish peroxidase-conjugated secondary antibody. An ECL-Plus system (GE Healthcare) was used to detect the protein signal (12). The expression level was determined by measuring the corresponding band intensities using ImageJ software, and the relative values were expressed relative to the α-tubulin signal.

Measurement of intracellular cAMP. NRVMs (2×10^5 cells/well in 24-well plate) were stimulated with the recombinant CTRP9 protein (10 μg/ml) or vehicle for 10 min. Intracellular cyclic AMP (cAMP) levels in NRVMs and myocardial tissue were determined with an enzyme immunoassay kit (GE Healthcare, NJ) according to the manufacturer's instructions.

Histological analysis. Tissue samples were embedded in OCT compound (Miles, Elkhart, IN) and snap-frozen in liquid nitrogen. Tissue

slices (6 μm) were prepared and stained with either anti-mouse CD45 antibodies (BD Biosciences) for evaluation of infiltrating immune cells, dihydroethidium (DHE; Wako) for evaluation of the superoxide production, or Masson trichrome for evaluation of the extent of tissue fibrosis.

To detect apoptosis, terminal deoxynucleotidyltransferase-mediated dUTP nick-end labeling (TUNEL) staining for the frozen heart sections was performed using an *in situ* cell death detection kit (Roche Diagnostics).

Statistical analysis. Data are presented as means ± the standard errors of the mean (SEM). A Student *t* test was performed for comparison between two independent groups. A one-way analysis of variance test was performed to compare three or more independent groups. A *P* value of <0.05 denoted the presence of a statistically significant difference.

RESULTS

Characteristics of CTRP9-KO mice. To investigate the role of endogenous CTRP9 in control of cardiac injury, we generated CTRP9-KO mice in a background of C57BL/6 mice. Plasma CTRP9 protein was undetectable in homozygous CTRP9-KO mice (Fig. 1A). The CTRP9 transcript was also undetectable in epididymal fat in homozygous CTRP9-KO mice. Under baseline conditions, there were no differences in body weight (BW), the tissue weights of brown fat, subcutaneous fat, epididymal fat, liver, heart, and lung, tibial length (TL), heart weight (HW)/BW, and HW/TL between CTRP9-KO and littermate wild-type (WT) mice at the age of 12 weeks (Table 1). In addition, there were no significant differences in systolic blood pressure, diastolic blood pressure, heart rate, and fasting blood glucose levels between the two strains of mice. Thus, CTRP-9-KO mice are indistinguishable from WT mice at the age of 12 weeks under basal conditions.

CTRP9-KO mice exhibit enhanced cardiac dysfunction in a model of endotoxinemia. To investigate the effect of CTRP9 on endotoxin-induced cardiac dysfunction, we intraperitoneally injected a single dose of LPS (10 mg/kg) or vehicle into CTRP9-KO or WT mice. LPS injection significantly reduced plasma CTRP9 levels in WT mice by 36% ± 18% compared to vehicle treatment. LPS injection also resulted in a significant reduction in CTRP9 mRNA expression in fat tissue (Fig. 1B). Figure 1C shows representative M-mode echocardiograms for CTRP9-KO and WT mice at 6 h after LPS injection. Echocardiographic analysis showed that LPS injection led to a decrease in the %FS in both strains of mice, but the CTRP9-KO mice showed a further decrease in %FS compared to WT mice (Fig. 1C). There was no significant difference in the %FS between CTRP9-KO and WT mice after injection of vehicle. We also investigated the effect of CTRP9 on diastolic function after LPS injection, as evaluated by the ratio of peak velocity of early to late filling of mitral inflow (E/A ratio) using transthoracic echocardiography. LPS injection led to an increase in the E/A ratio in both WT and CTRP9-KO mice, but the CTRP9-KO mice showed a further increase in the E/A ratio compared to WT mice (Fig. 1D), a finding indicative of severe diastolic dysfunction.

We next assessed whether overproduction of CTRP9 modulates LPS-mediated LV contractile dysfunction. WT mice were systemically treated with Ad-CTRP9 or Ad-β-gal via tail vein injection prior to LPS delivery. Ad-CTRP9-treated WT mice showed a (3.3 ± 0.4)-fold increase in plasma levels of CTRP9 at 3 days after adenoviral injection compared to Ad-β-gal-treated WT mice. At 5 days after adenoviral vector delivery, WT mice receiving Ad-CTRP9 showed a significantly increased %FS after LPS injection compared to WT mice treated with the Ad-β-gal (Fig. 1E). WT mice receiving Ad-CTRP9 also showed a significant decrease in the E/A ratio after LPS injection compared to WT mice treated with Ad-β-gal (2.06 ± 0.07 in the Ad-β-gal group versus 1.77 ± 0.02 in the Ad-CTRP9 group; $P < 0.05$).

Because inflammatory response and oxidative stress are associated with the development of cardiac injury and dysfunction in sepsis-induced cardiac dysfunction and other models of cardiac injury (21–23), mRNA levels of proinflammatory cytokines and NADPH oxidase components in the myocardium in CTRP9-KO and WT mice at 6 h after LPS administration were measured by real-time PCR methods. CTRP9-KO mice showed higher expression levels of proinflammatory cytokines, including TNF-α, IL-6, IL-1β, and MCP-1, and NADPH oxidase components, including $gp91^{phox}$, $p67^{phox}$, and $p47^{phox}$, compared to WT mice (Fig. 1F). At 6 h after LPS administration, CTRP9-KO mice showed higher plasma TNF-α levels compared to WT mice (Fig. 1G). LPS injection also increased the number of CD45-positive infiltrating immune cells in the heart tissue to a greater extent in CTRP9-KO mice than in WT mice (76.8 ± 0.4 U/field in WT mice versus 123.7 ± 9.1 U/field in CTRP9-KO mice, $P < 0.05$) (Fig. 1H). To investigate the production of ROS in the heart, we performed dihydroethidium (DHE) staining by fluorescence microscopy. LPS injection increased the ROS production in the heart tissue to a greater extent in CTRP9-KO mice than in WT mice (Fig. 1I). Thus, the loss of CTRP9 exacerbates acute cardiac injury after LPS injection, which is accompanied by increased inflammatory state and oxidative stress.

CTRP9-KO mice exhibit increased infarct size and inflammatory response in the heart after ischemia-reperfusion. To investigate the role of endogenous CTRP9 in cardiac ischemic injury, CTRP9-KO and WT mice were subjected to 60 min of LAD vessel ligation, followed by 24 h of reperfusion. Representative photographs of myocardial tissues after staining with Evans blue dye to delineate AAR and 2,3,5-triphenyltetrazolium chloride to delineate IA in WT and CTRP9-KO mice are shown in Fig. 2A. The area-at-risk/left-ventricular (AAR/LV) ratio was the same in CTRP9-KO and WT mice (Fig. 2A). However, the IA/AAR and IA/LV ratios in CTRP9-KO mice were increased by 20.2% ± 4.2% and 24.5% ± 1.9%, respectively, compared to those of WT mice (Fig. 2A). Echocardiographic analysis showed that myocardial ischemia-reperfusion injury led to a decrease in %FS in both WT and CTRP9-KO mice, but the CTRP9-KO mice showed a further decrease in %FS compared to WT mice (Fig. 2B). Ischemia-reperfusion also resulted in an increase in the E/A ratio in both strains of mice, but this induction was further enhanced in CTRP9-KO mice compared to WT mice (2.32 ± 0.19 in WT mice versus 3.35 ± 0.28 in CTRP9-KO mice, $P < 0.01$).

To investigate the extent of apoptosis in the AAR regions, TUNEL staining was performed. Quantitative analysis revealed a significantly higher proportion of TUNEL-positive cells in the myocardium of CTRP9-KO mice compared to WT mice after ischemia-reperfusion injury, whereas few or no TUNEL-positive cells could be detected in the myocardium of WT or CTRP9-KO mice after a sham operation (Fig. 2C). Minimal interstitial fibrosis in the part other than infarct area was detected in hearts of CTRP-KO and WT mice after ischemia-reperfusion injury, and no significant differences were observed in interstitial fibrotic areas between CTRP-KO and WT mice (data not shown).

The cardiac levels of TNF-α and IL-6 were assessed by real-time PCR methods. Ischemia-reperfusion led to increases in TNF-α and IL-6 mRNA levels in WT mice, a finding consistent

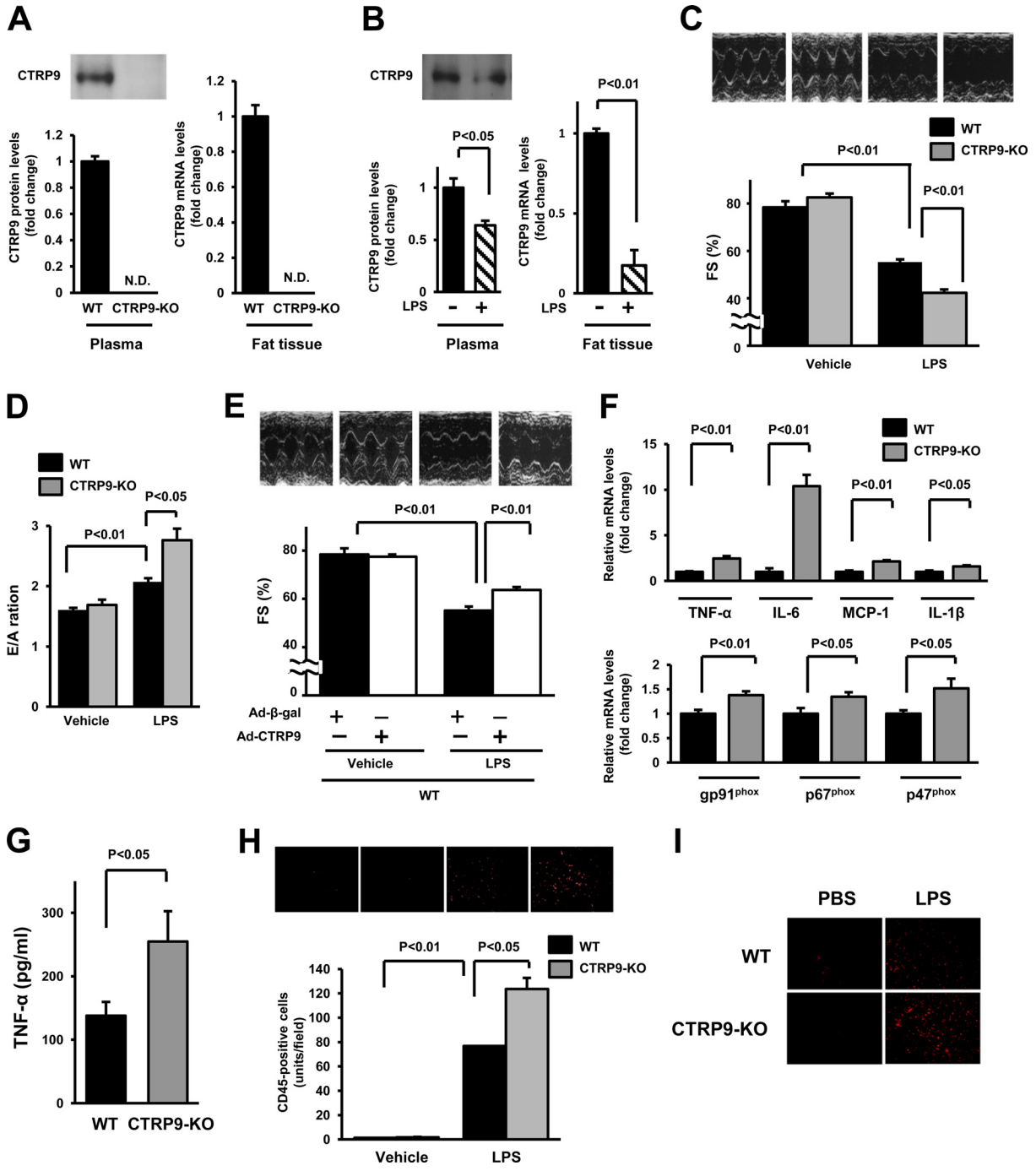

FIG 1 Loss of CTRP9 results in exacerbated LPS-induced cardiac dysfunction and inflammation. (A) CTRP9 expression in plasma and fat tissue in WT and CTRP9-KO mice. Plasma CTRP9 levels were assessed by Western blotting (left). CTRP9 mRNA levels were determined in fat tissue of WT and CTRP9-KO mice by real-time PCR methods (right) ($n = 4$ in each group). (B) CTRP9 expression in plasma and fat tissue in WT mice after injection of LPS or vehicle. (C) Representative M-mode echocardiograms for WT and CTRP9-KO mice 6 h after LPS or control vehicle injection (upper). Quantitative analysis of the fractional shortening (FS) in WT and CTRP9-KO mice 6 h after LPS or vehicle injection ($n = 5$ in each group) (lower). (D) Quantitative analysis of the ratio of peak velocity of early to late filling of mitral inflow (E/A ratio) in WT and CTRP9-KO mice 6 h after injection of LPS or vehicle ($n = 5$ in each group). (E) Representative M-mode echocardiograms 6 h after LPS or vehicle injection in WT mice pretreated with Ad-CTRP9 or Ad-β-gal (upper). Quantitative analysis of the %FS 6 h after LPS injection in WT mice pretreated with Ad-CTRP9 or Ad-β-gal (lower). Ad-CTRP9 or Ad-β-gal (3.0×10^8 PFU total) was delivered intravenously via the tail vein 5 days before LPS or vehicle injection ($n = 8$ in each group). (F) mRNA levels of TNF-α, IL-6, MCP-1, IL-1β, $gp91^{phox}$, $p67^{phox}$, and $p47^{phox}$ in the myocardia in CTRP9-KO and WT mice at 6 h after LPS administration. mRNA levels were measured by real-time PCR method ($n = 6$ in each group). All results are normalized to β-actin. (G) Serum levels of TNF-α in CTRP9-KO and WT mice at 6 h after LPS administration. (H) Infiltrating immune cells in the heart of CTRP9-KO and WT mice. Fluorescence staining of heart tissues with anti-CD45 antibody (red) is shown in upper panels. Quantitative analysis of CD45-positive cells in the heart of CTRP9-KO ($n = 5$) and WT ($n = 5$) mice at 6 h after administration of LPS or vehicle is shown in lower panel. CD45-positive cells were counted in several randomly selected fields and expressed as the number of CD45-positive cells per high power field (×400, middle panel). (I) Production of reactive oxygen species as evaluated by immunostaining with dihydroethidium (×400 each field; red). The results are presented as means ± the SEM.

TABLE 1 Morphometric and hemodynamic parameters of CTRP9-KO mice

Parameter	Mean ± SEM		*P*
	WT	CTRP9-KO	
BW (g)	24.6 ± 0.6	23.9 ± 0.4	0.49
sBP (mm Hg)	107.4 ± 1.7	105.4 ± 5.0	0.72
dBP (mm Hg)	60.7 ± 5.7	51.6 ± 3.0	0.20
HR (bpm)	561.9 ± 22.4	611.1 ± 11.0	0.08
FBS (mg/dl)	72.3 ± 6.9	68.4 ± 2.7	0.62
BAT (mg)	40.8 ± 3.8	44.6 ± 8.7	0.70
Sub fat (mg)	184.2 ± 27.4	152.9 ± 7.9	0.31
Epi fat (mg)	196.2 ± 28.5	205.3 ± 9.7	0.77
Liver (mg)	922.6 ± 24.9	949.0 ± 60.0	0.70
Heart (mg)	110.2 ± 8.5	117.6 ± 4.6	0.46
Lung (mg)	134.3 ± 7.3	143.4 ± 3.4	0.29
Tibial length (mm)	21.1 ± 0.5	20.2 ± 0.6	0.25
HW/BW (mg/g)	4.5 ± 0.2	4.9 ± 0.1	0.13
HW/TL (mg/mm)	5.2 ± 0.3	5.8 ± 0.2	0.13

[a] BW, body weight; sBP, systolic blood pressure; dBP, diastolic blood pressure; HR, heart rate; FBS, fasting blood sugar; BAT, brown adipose tissue; Sub, subcutaneous; Epi, epididymal; HW, heart weight; TL, tibial length.

with previous reports (19, 24), but the magnitude of this induction was much greater in CTRP9-KO than in WT mice (Fig. 2D). Basal cardiac expression of TNF-α and IL-6 in sham-operated hearts did not significantly differ between CTRP9-KO and WT mice. In addition, ischemia-reperfusion injury increased the number of $CD45^+$ cells in the heart tissue to a greater extent in CTRP9-KO mice than in WT mice (Fig. 2E). No significant differences were observed in the number of $CD45^+$ cells in the myocardium between WT and CTRP9-KO mice after sham operation. Therefore, these data show that CTRP9 acts as an endogenous modulator that protects the heart from acute damage and inflammatory responses.

CTRP9 attenuates inflammatory response in cardiac myocytes. To examine the effect of CTRP9 on inflammatory response to LPS at a more mechanistic level, cultured cardiac myocytes were pretreated with CTRP9 protein of vehicle and subjected to LPS or PBS stimulation for 6 h. The transcript levels of TNF-α and IL-6 in cardiac myocytes were measured by real-time PCR methods. Exposure to LPS increased mRNA expression of TNF-α and IL-6 in cardiac myocytes, and pretreatment with CTRP9 protein significantly reduced LPS-induced expression of each of these transcripts (Fig. 3A).

The transcription factor, NF-κB, is a key mediator of inflammatory responses in various cells, including cardiac myocytes (25). Thus, we assessed the effect of CTRP9 on NF-κB phosphorylation in response to LPS. Stimulation of cardiac myocytes with LPS resulted in a time-dependent increase in NF-κB phosphorylation, and CTRP9 pretreatment significantly suppressed LPS-stimulated NF-κB phosphorylation (Fig. 3B). Correspondingly, CTRP9-KO mice exhibited an increased level of NF-κB phosphorylation in the heart after LPS treatment compared to WT mice (Fig. 3C). Ad-CTRP9 treatment significantly attenuated LPS-induced increase in NF-κB phosphorylation in the hearts of WT mice *in vivo*, but Ad-CTRP9 had no effect on NF-κB phosphorylation in the hearts of PBS-treated WT mice (Fig. 3D). Ad-CTRP9 treatment also reversed LPS-induced reduction in IκB-α protein expression in the hearts of WT mice *in vivo* (Fig. 3D). In contrast, Ad-CTRP9 had no effect on IκB-α level in the hearts of vehicle-treated WT mice.

To analyze the involvement of NF-κB activation in cardiac phenotypes of CTRP9-KO mice *in vivo*, WT and CTRP9-KO mice were treated with the NF-κB inhibitor, PDTC, by intraperitoneal injection, followed by stimulation with LPS. Treatment with PDTC significantly increased the %FS in WT mice after LPS injection. PDTC treatment reversed the reduction of the %FS in LPS-stimulated CTRP9-KO mice to the levels similar to those observed in LPS-treated WT mice after PDTC administration (Fig. 3E). These data suggest that NF-κB activation in response to LPS contributes to cardiac dysfunction observed in CTRP9-KO mice.

AMPK is essential for the anti-inflammatory effects of CTRP9 in cardiac myocytes. CTRP9 has been shown to promote AMPK signaling in cultured cells, including cardiac myocytes (10, 12). To assess the potential contribution of AMPK signaling to the anti-inflammatory actions of CTRP9, myocytes were transduced with Ad-dn-AMPK or Ad-β-gal and treated with CTRP9 protein or vehicle, followed by exposure to LPS or PBS. Transduction with Ad-dn-AMPK abolished CTRP9-stimulated phosphorylation of ACC, a downstream target of AMPK in cardiac myocytes (Fig. 4A). Transduction with Ad-dn-AMPK also abrogated the suppressive actions of CTRP9 on LPS-stimulated mRNA expression of TNF-α and IL-6 in cardiac myocytes (Fig. 4B).

Because CTRP9 increases cAMP levels in vascular smooth muscle cells (11), we investigated whether CTRP9 affects cAMP contents in cardiac myocytes. Treatment of cardiac myocytes with CTRP9 increased the intracellular cAMP levels (Fig. 4C). We also assessed cAMP levels in the heart from CTRP9-KO and WT mice. LPS injection reduced cAMP concentrations in the hearts in both WT and CTRP9-KO mice, but the CTRP9-KO mice showed a further decrease in myocardial cAMP levels compared to WT mice after LPS treatment (Fig. 4D).

To examine the possible participation of cAMP in anti-inflammatory effects of CTRP9 in cardiac myocytes, cells were pretreated with the adenylate cyclase inhibitor SQ22536 or vehicle and cultured in the presence or absence of CTRP9 protein, followed by stimulation with LPS or PBS. Pretreatment with SQ22536 partially reversed the inhibitory effect of CTRP9 on LPS-stimulated expression of TNF-α and IL-6 in myocytes (Fig. 4E). Furthermore, pretreatment with SQ22536 reversed the inhibitory actions of CTRP9 on LPS-induced NF-κB phosphorylation in cardiac myocytes (Fig. 4F).

We also assessed the contribution of AMPK to CTRP9-mediated suppression of NF-κB phosphorylation by transduction with Ad-dn-AMPK. Transduction with Ad-dn-AMPK reversed the inhibitory actions of CTRP9 on LPS-induced NF-κB phosphorylation in cardiac myocytes (Fig. 4G). Pretreatment with the AMPK inhibitor, compound C, also blocked CTRP9-mediated inhibition of LPS-stimulated NF-κB phosphorylation in cardiac myocytes (Fig. 4F).

AMPK is involved in the protective effects of CTRP9 on acute cardiac injury *in vivo*. To test the role of AMPK in CTRP9-mediated cardioprotection *in vivo*, the phosphorylation of AMPK was assessed by Western blotting in the hearts of CTRP9-KO and WT mice. Administration of LPS increased the phosphorylation levels of AMPK and ACC in WT hearts, but these inductions were significantly attenuated in the myocardia of CTRP9-KO mice (Fig. 5A). The low basal level of AMPK phosphorylation in the heart did not differ between vehicle-treated CTRP9-KO and WT mice.

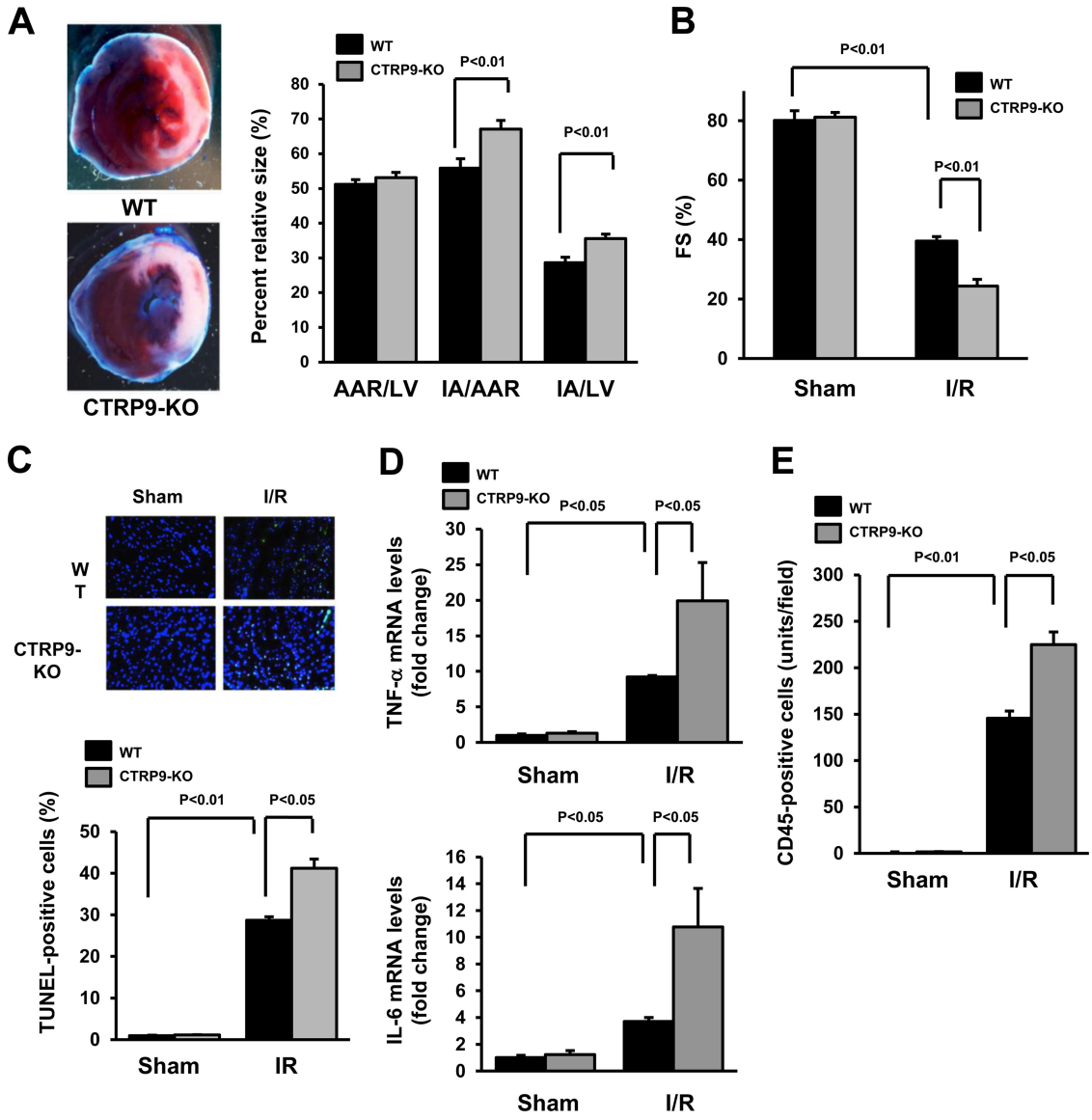

FIG 2 CTRP-KO mice show increased myocardial infarct size and inflammatory response following ischemia-reperfusion injury. (A) Representative pictures of myocardial tissues from WT and CTRP9-KO mice at 24 h after ischemia-reperfusion (I/R) (left). The nonischemic area is indicated by blue, the area at risk (AAR) is indicated by red, and the infarct area (IA) is indicated by white. Quantification of the LV area, the AAR, and the IA in WT ($n = 7$) and CTRP9-KO ($n = 6$) mice is shown (right). (B) Quantitative analysis of the fractional shortening (FS) in WT and CTRP9-KO mice at 24 h after sham or I/R surgery ($n = 5$ in each group). (C) Representative photographs of heart sections stained with TUNEL from CTRP9-KO and WT mice at 24 h after sham or I/R surgery (upper panels). Apoptotic nuclei were determined by TUNEL staining (green), and total nuclei were counterstained with DAPI (blue). Results for the quantitative analysis of apoptotic nuclei from the hearts of CTRP9-KO and WT mice after sham or I/R operation are shown in the lower panel. TUNEL-positive nuclei were counted in several randomly selected fields, and the results are expressed as a percentage of the total number of nuclei. (D) Cardiac expression of TNF-α and IL-6 in WT ($n = 5$) and CTRP9-KO ($n = 5$) mice at 24 h after sham or I/R operation. The mRNA levels of TNF-α and IL-6 in the myocardia of WT and CTRP9-KO mice were quantified by real-time PCR method and are expressed relative to the β-actin mRNA levels. (E) Quantitative analysis of CD45-positive cells in the ischemic hearts of CTRP9-KO ($n = 5$) and WT ($n = 5$) mice at 24 h after sham or I/R surgery. The results are presented as means ± the SEM.

Moreover, Ad-CTRP9 treatment significantly enhanced LPS-induced increase in AMPK phosphorylation in the hearts of WT mice (Fig. 5B). Ad-CTRP9 had no effects on AMPK phosphorylation in the hearts of PBS-treated WT mice (data not shown).

To analyze the involvement of AMPK signaling in the cardioprotective action of CTRP9 *in vivo*, WT and muscle-specific dnAMPK-TG mice that had received an intravenous injection of Ad-CTRP9 or Ad-β-gal were treated with LPS. The absence of AMPK phosphorylation at residue Thr172 in the heart of dnAMPK-TG mice was confirmed (data not shown). The dnAMPK-TG mice treated with Ad-CTRP9 exhibited a (2.3 ± 0.5)-fold increase in plasma CTRP9 level at 3 days after adenoviral injection compared to Ad-β-gal-treated mice. Administration of Ad-CTRP9 enhanced ACC phosphorylation in LPS-treated WT hearts, but this increase was significantly attenuated in LPS-treated hearts of dnAMPK-TG mice (Fig. 5C). The dnAMPK-TG mice exhibited a decreased %FS compared to WT mice following LPS injection (Fig. 5D). In contrast to

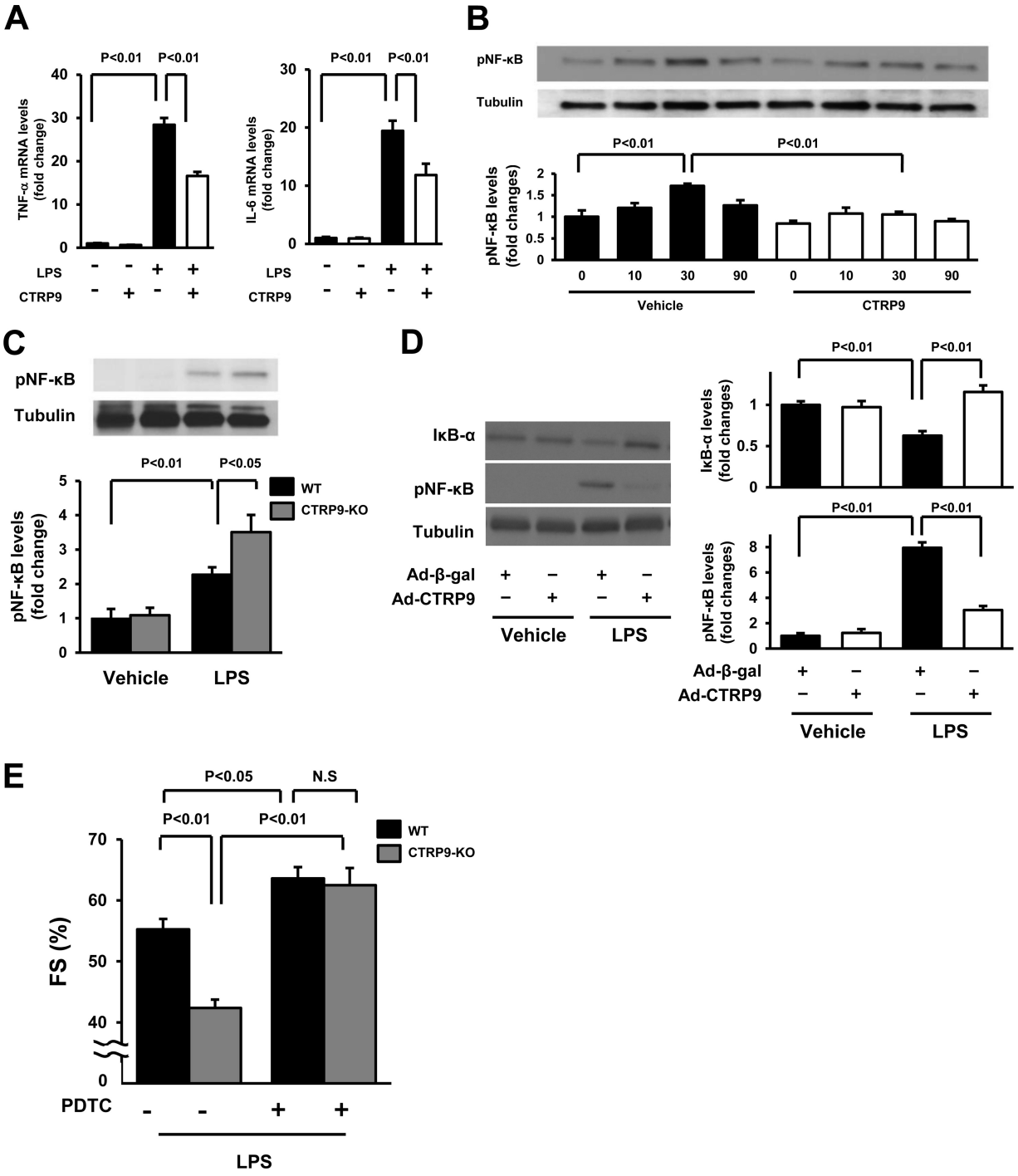

FIG 3 CTRP9 suppresses the inflammatory response to LPS in cultured cardiac myocytes. (A) Effect of CTRP9 on LPS-induced expression of TNF-α (left) and IL-6 (right) in cardiac myocytes. Cells were pretreated with CTRP9 (10 μg/ml) or vehicle for 4 h and stimulated with or without LPS (100 ng/ml) for 6 h. The mRNA expression of TNF-α and IL-6 was measured by real-time PCR method and expressed relative to β-actin levels ($n = 6$). (B) Effect of CTRP9 on NF-κB phosphorylation in response to LPS. Cells were pretreated with CTRP9 (10 μg/ml) or vehicle for 4 h followed by stimulation with LPS (100 ng/ml) or vehicle for the indicated length of time ($n = 3$). Phosphorylation of NF-κB (pNF-κB) was determined by Western blotting. The phosphorylation level was determined by measuring the corresponding band intensities using ImageJ software, and the relative values were expressed relative to the α-tubulin signals. (C) Phosphorylation of NF-κB in the hearts of CTRP9-KO and WT mice at 6 h after injection of LPS or vehicle, as assessed by Western blotting. (D) NF-κB phosphorylation and IκB-α protein expression in the heart of mice treated with Ad-CTRP9 or Ad-β-gal at 6 h after LPS or vehicle injection. WT mice were systemically treated with Ad-CTRP9 or Ad-β-gal (3.0×10^8 PFU total) 5 days before LPS or vehicle injection. (E) Quantitative analysis of the %FS after treatment with the NF-κB inhibitor, PDTC, or vehicle in CTRP9-KO and WT mice at 6 h after LPS injection ($n = 5$ in each group). PDTC (100 mg/kg) or vehicle was given by intraperitoneal injection in CTRP9-KO and WT mice 1 h before LPS treatment. The results are presented as the means ± the SEM.

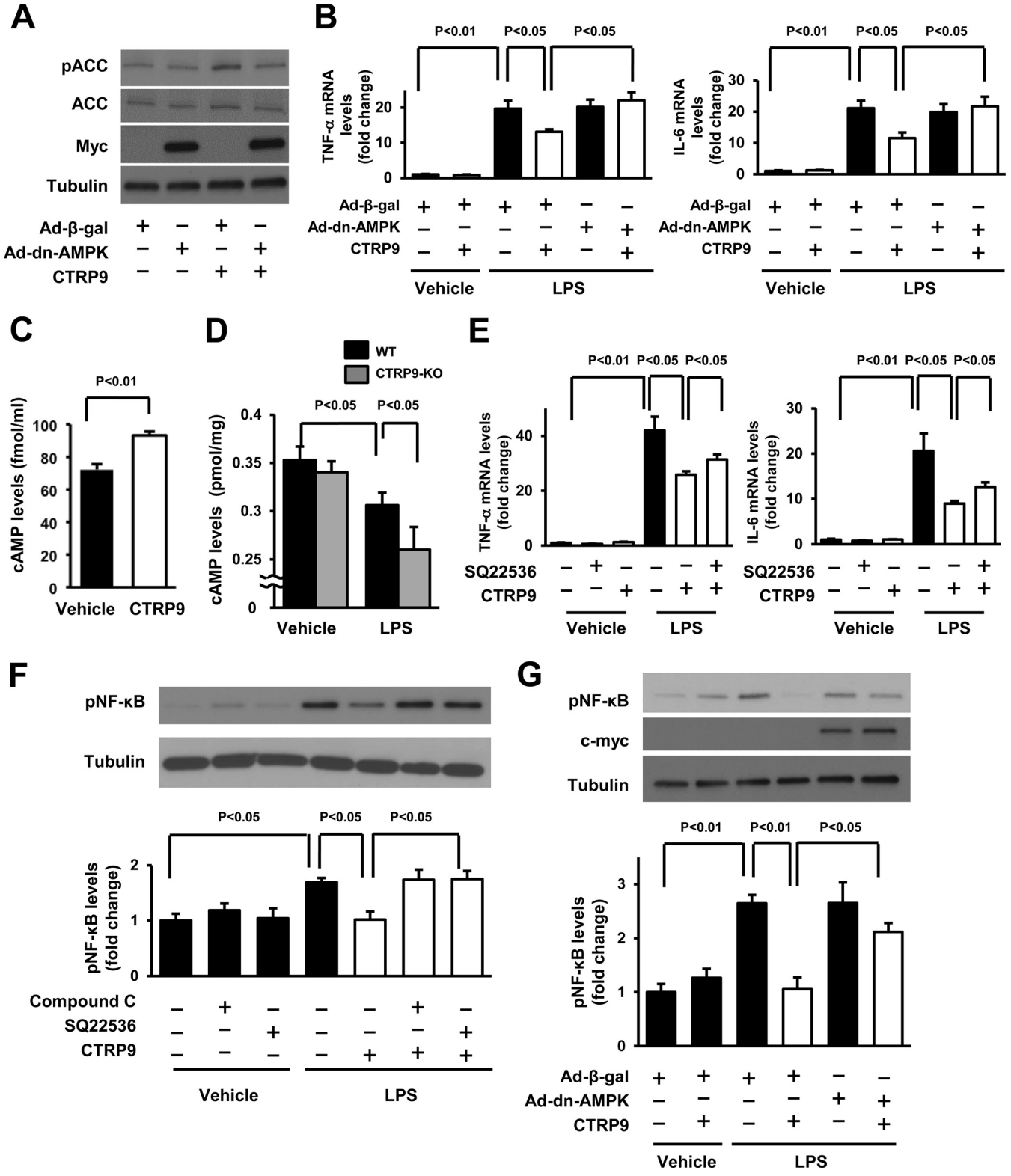

FIG 4 AMPK-dependent inhibition of cardiac inflammation by CTRP9 *in vitro*. (A) Effect of AMPK inactivation on CTRP9-stimulated phosphorylation of ACC. After transduction with an c-myc-tagged Ad-dn-AMPK or Ad-β-gal at an MOI of 10 for 24 h, cardiac myocytes were treated with CTRP9 (10 μg/ml) or vehicle for 15 min. (B) AMPK participates in the inhibitory effect of CTRP9 on LPS-induced expression of TNF-α and IL-6. After transduction with an Ad-dn-AMPK or Ad-β-gal at an MOI of 10 for 24 h, cardiac myocytes were treated with CTRP9 (10 μg/ml) or vehicle for 4 h, followed by stimulation with LPS (100 ng/ml) or vehicle for 6 h. The mRNA levels were analyzed by real-time PCR method and expressed relative to the β-actin levels ($n = 6$ in each group). (C) Intracellular cAMP production in cardiac myocytes after stimulation with CTRP9. Cells were stimulated with CTRP9 protein (10 μg/ml) or vehicle for 10 min. (D) Myocardial cAMP levels in CTRP9-KO and WT mice at 6 h after administration of LPS or vehicle. (E) Contribution of cAMP signal to the inhibitory effects

WT mice, Ad-CTRP9 did not affect %FS in dnAMPK-TG mice after LPS injection (Fig. 5D). In addition, dnAMPK-TG mice showed increased mRNA levels of TNF-α and IL-6 in the heart compared to WT mice following LPS injection ($P < 0.05$) (Fig. 5E). Ad-CTRP9 treatment had no effects on TNF-α and IL-6 expression in the hearts of LPS-treated dnAMPK-TG mice (Fig. 5E). These data support the notion that CTRP9 suppresses myocardial dysfunction and inflammatory response to LPS via activation of AMPK in cardiac myocytes.

AdipoR1 is involved in the cardioprotective action of CTRP9 *in vivo*. AdipoR1 contributes to the actions of CTRP9 on AMPK activation *in vitro* (10, 12). To test the possible involvement of AdipoR1 in CTRP9-induced inhibition of the inflammatory response to LPS, cardiac myocytes were transfected with siRNAs targeting AdipoR1 or AdipoR2 or with unrelated siRNAs, followed by stimulation with CTRP9 or vehicle. Transfection of cardiac myocytes with siRNAs targeting AdipoR1 or AdipoR2 resulted in reduction of AdipoR1 and AdipoR2 mRNA levels by 85 and 77%, respectively. Ablation of AdipoR1, but not knockdown of AdipoR2, suppressed CTRP9-induced increase in AMPK phosphorylation (Fig. 6A) in agreement with our previous report (12). Knockdown of AdipoR1, but not the deletion of AdipoR2, reversed the inhibitory effect of CTRP9 on LPS-stimulated expression of TNF-α and IL-6 in myocytes (Fig. 6B).

To analyze the involvement of AdipoR1 in the cardioprotective action of CTRP9 *in vivo*, AdipoR1-KO mice that received an intravenous infusion of Ad-CTRP9 or Ad-β-gal were stimulated with LPS or PBS. Plasma levels of CTRP9 did not differ between AdipoR1-KO and WT mice under basal conditions (Fig. 6C). Ad-CTRP9 treatment increased plasma CTRP9 levels in AdipoR1-KO mice by a factor of 2.0 ± 0.1 at 3 days after adenoviral injection compared to Ad-β-gal treatment. Ad-CTRP9 stimulated AMPK phosphorylation in LPS-treated WT hearts, but CTRP9-induced phosphorylation of AMPK was diminished in LPS-treated AdipoR1-KO hearts (Fig. 6D). AdipoR1-KO mice showed decreased the %FS following LPS injection, and treatment with Ad-CTRP9 did not affect the LPS-induced reduction of the %FS in AdipoR1-KO mice (Fig. 6E). Likewise, Ad-CTRP9 treatment did not affect the E/A ratio in vehicle-treated AdipoR1-KO mice compared to Ad-β-gal (1.57 ± 0.07 in the Ad-β-gal group versus 1.67 ± 0.02 in the Ad-CTRP9 group). AdipoR1-KO mice receiving Ad-β-gal showed the increase in the E/A ratio following LPS injection, and Ad-CTRP9 had no effects on the E/A ratio in LPS-treated AdipoR1-KO mice compared to Ad-β-gal (2.35 ± 0.09 in the Ad-β-gal group versus 2.47 ± 0.21 in the Ad-CTRP9 group). TUNEL-positive cells and interstitial fibrosis areas were rarely detected in the hearts of AdipoR1-KO mice treated with Ad-β-gal or Ad-CTRP9 at 6 h after injection of LPS or vehicle (data not shown).

Moreover, AdipoR1-KO mice exhibited an increase in cardiac TNF-α and IL-6 mRNA expression compared to WT mice after LPS injection (Fig. 6F). Ad-CTRP9 had no effects on TNF-α and IL-6 expression in the hearts of AdipoR1-KO mice after LPS stimulation. Ad-CTRP9 also had no effects on the number of CD45-positive cells in the hearts of AdipoR1-KO mice after LPS stimulation (124.2 ± 7.0 U/field in the Ad-β-gal group versus 126.1 ± 6.7 U/field in Ad-CTRP9 group).

DISCUSSION

The present study provides the first evidence that endogenous CTRP9 confers resistance to myocardial injury responses in established mouse models of acute cardiac damage. In a model of sepsis-associated myocardial dysfunction, CTRP9-KO mice showed greater LV systolic and diastolic dysfunction following LPS administration compared to WT mice. CTRP9-KO mice also showed increased infarct size and exacerbated cardiac function following ischemia-reperfusion compared to WT mice. These data document, for the first time, that endogenous CTRP9 functions to protect the heart from pathological stresses. In this regard, it has been shown that obesity is associated with reduced levels of circulating CTRP9 (6). Given that obesity-related disorders are implicated in the severity and worse outcome of heart diseases (1, 2), these data suggest that reductions in CTRP9 levels could contribute to obesity-linked cardiac disease.

Here, we also showed that the systemic delivery of CTRP9 using an adenoviral vector alleviated the LPS-induced LV dysfunction in mice. Previously, we showed that treatment with CTRP9 protein ameliorates myocardial injury after ischemia-reperfusion (12). Thus, CTRP9 can be protective against the development of cardiac damage and dysfunction in response to various pathological stimuli. Taken together, these data indicate that approaches to restore or increase circulating CTRP9 levels under conditions of obesity could be beneficial for the prevention of acute cardiac injury.

Inflammatory responses exacerbate cardiac injury and dysfunction after ischemia-reperfusion or LPS challenge (21, 22). Our data showed that CTRP9-KO mice had increased levels of proinflammatory cytokines and infiltrating immune cells in the myocardium following injury. Conversely, administration of CTRP9 to WT mice led to reduction of myocardial expression of proinflammatory genes after LPS stimulation. CTRP9 also reduced proinflammatory gene expression in cultured cardiac myocytes treated with LPS. Thus, it is likely that CTRP9 protects against various cardiac injuries via the suppression of inflammatory reactions.

Our data indicate that CTRP9 attenuates the inflammatory response to acute cardiac injury, at least in part, through its ability to activate AMPK signaling in cardiac myocytes. CTRP9 positively

of CTRP9 on LPS-stimulated expression of TNF-α and IL-6 in cardiac myocytes. Cells were pretreated with adenylate cyclase inhibitor SQ22536 (SQ; 10 μmol/liter) or vehicle (DMSO) for 60 min and then treated with or without CTRP9 (10 μg/ml) for 4 h, followed by stimulation with LPS (100 ng/ml) or vehicle for 6 h. The mRNA levels were analyzed by real-time PCR method and expressed relative to β-actin levels ($n = 6$ in each group). (F and G) Involvement of AMPK and cAMP in the suppressive effects of CTRP9 on LPS-stimulated phosphorylation of NF-κB in cardiac myocytes. (F) Cells were pretreated with the AMPK inhibitor, compound C (10 μmol/liter), SQ22536 (10 μmol/liter), or vehicle (DMSO) for 60 min and then treated with or without CTRP9 (10 μg/ml) for 4 h, followed by stimulation with LPS (100 ng/ml) or vehicle for 30 min. (G) After transduction with a c-myc-tagged Ad-dn-AMPK or Ad-β-gal at an MOI of 10 for 24 h, cardiac myocytes were treated with CTRP9 (10 μg/ml) or vehicle for 4 h, followed by stimulation with LPS (100 ng/ml) or vehicle for 30 min. Phosphorylation of NF-κB (pNF-κB) was determined by Western blotting. The phosphorylation level was determined by measurement of the corresponding band intensities by using ImageJ software, and the relative values were expressed relative to α-tubulin signals. The results are presented as the means ± the SEM ($n = 3$ in each group).

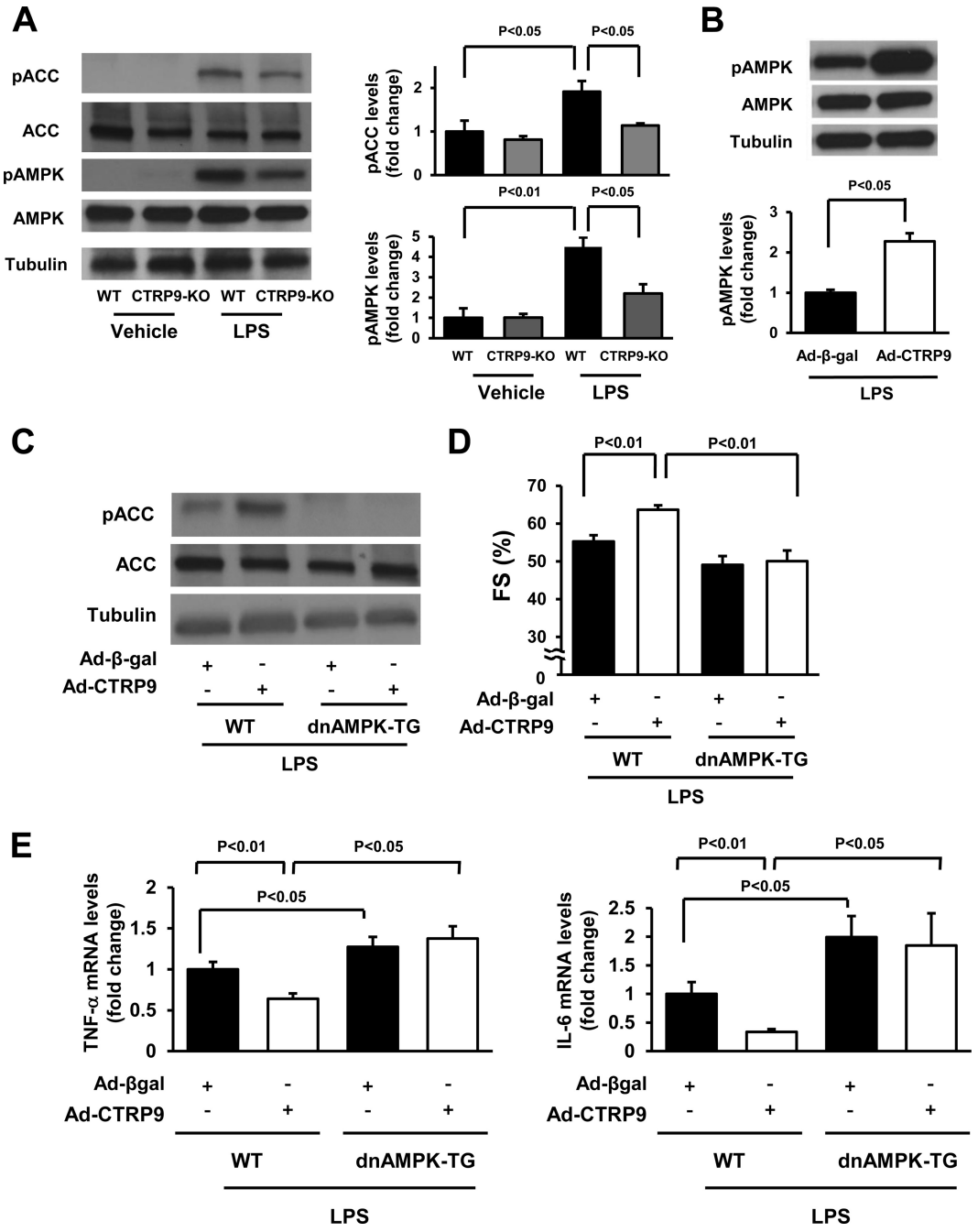

FIG 5 AMPK is involved in the protective effects of CTRP9 on myocardial injury *in vivo*. (A) Phosphorylation of ACC and AMPK in the hearts of CTRP9-KO and WT mice 6 h after LPS or vehicle injection as assessed by Western blotting. (B) Phosphorylation levels of AMPK in the hearts of WT mice treated with Ad-CTRP9 or Ad-β-gal at 6 h after LPS injection. WT mice were systemically treated with Ad-CTRP9 or Ad-β-gal (3.0×10^8 PFU total), followed by subjection to LPS injection. (C) Phosphorylation of ACC in the hearts of WT and dnAMPK-TG mice receiving Ad-CTRP9 or Ad-β-gal at 6 h after LPS injection. Ad-CTRP9 or Ad-β-gal (3.0×10^8 PFU total) was delivered intravenously via the tail vein 5 days before LPS injection. Phosphorylation of ACC (pACC) was determined by Western blotting. (D) Quantitative analysis of the %FS in WT and dnAMPK-TG mice receiving Ad-CTRP9 or Ad-β-gal at 6 h after LPS injection. Ad-CTRP9 or Ad-β-gal (3.0×10^8 PFU total) was delivered intravenously via the tail vein 5 days before LPS injection ($n = 8$ in each group). (E) Myocardial levels of TNF-α and IL-6 in WT ($n = 6$) and dnAMPK-TG ($n = 5$) mice at 6 h after LPS injection. mRNA levels of TNF-α and IL-6 were measured in the myocardium of WT and dnAMPK-TG mice that had received Ad-CTRP9 or Ad-β-gal by real-time PCR method and expressed relative to β-actin mRNA levels. The results are presented as means ± the SEM.

regulated AMPK activation in the heart in response to LPS. Of importance, these observations indicate that the beneficial action of CTRP9 on cardiac dysfunction and inflammation in response to LPS is abolished under conditions of AMPK inactivation in myocardium. Moreover, the anti-inflammatory actions of CTRP9 in LPS-treated cardiomyocytes are reversed by blockade of AMPK activation. These results are consistent with the previous observations that AMPK activation leads to reduced inflammatory re-

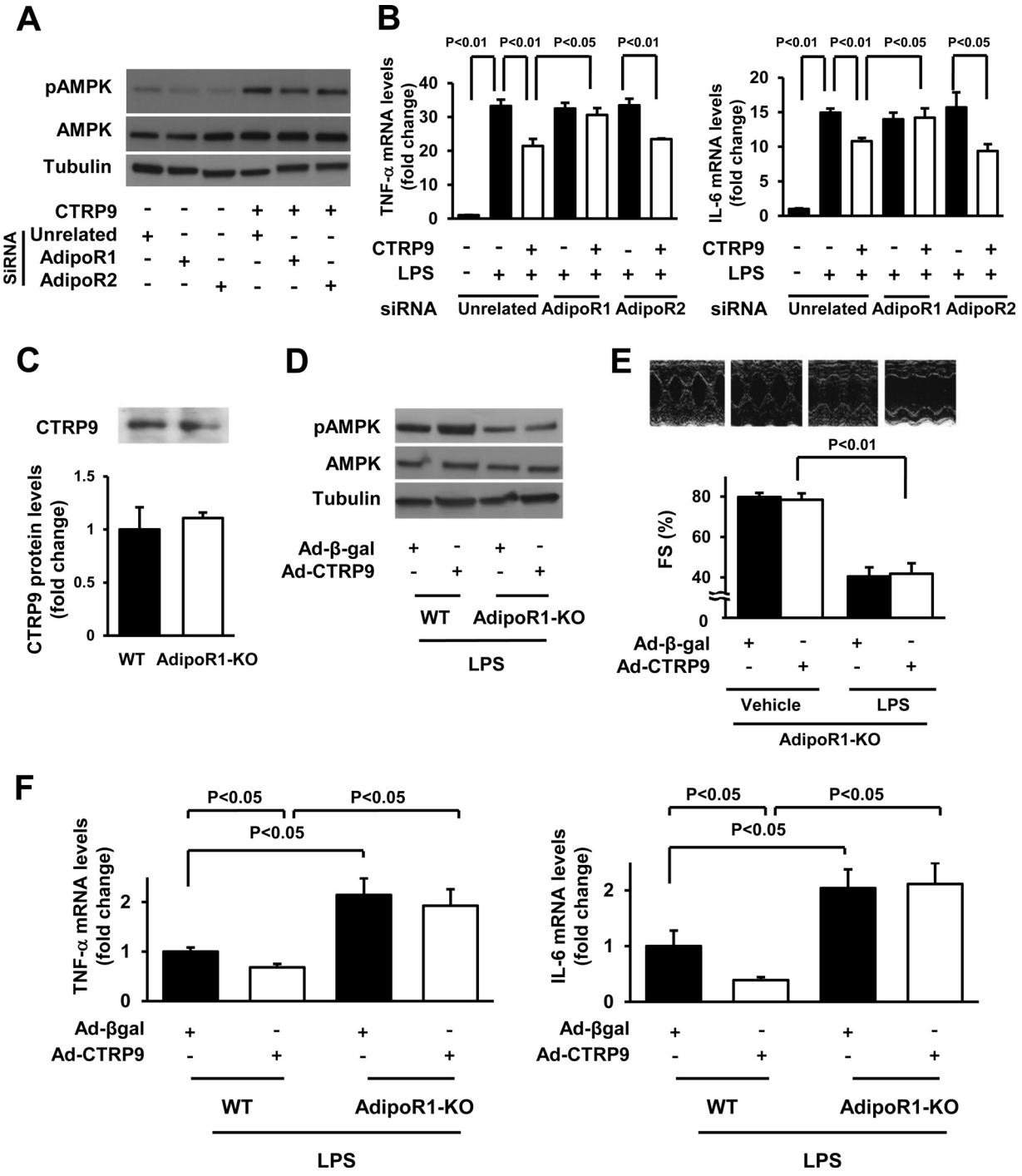

FIG 6 AdipoR1 contributes to the protective actions of CTRP9 on myocardial injury. (A) Effect of AdipoR1 ablation on CTRP9-stimulated phosphorylation of AMPK. Cardiac myocytes were transfected with siRNAs against AdipoR1 or AdipoR2 or unrelated siRNAs, followed by stimulation with CTRP9 protein (10 μg/ml) or vehicle for 15 min. (B) Role of adiponectin receptors in CTRP9-mediated inhibition of inflammatory response to LPS in cardiac myocytes. Cells were transfected with siRNAs against AdipoR1, AdipoR2, or unrelated siRNAs and then pretreated with CTRP9 (10 μg/ml) or vehicle for 4 h, followed by treatment with LPS (100 ng/ml) or vehicle for 6 h. The mRNA levels of TNF-α and IL-6 were analyzed by real-time PCR method and expressed relative to β-actin levels (n = 6 in each group). (C) Plasma CTRP9 levels of WT and AdipoR1-KO mice. Plasma CTRP9 levels were assessed by Western blotting (n = 4 in each group). (D) Phosphorylation of AMPK in the hearts of WT and AdipoR1-KO mice receiving Ad-CTRP9 or Ad-β-gal at 6 h after LPS injection. Ad-CTRP9 or Ad-β-gal (3.0×10^8 PFU total) was delivered intravenously via the tail vein 5 days before LPS injection. Phosphorylation levels of AMPK were determined by Western blotting. (E) Representative M-mode echocardiograms in WT and AdipoR1-KO mice receiving Ad-CTRP9 or Ad-β-gal at 6 h after LPS injection (upper). Quantitative analysis of the fractional shortening (FS) in WT and AdipoR1-KO mice treated with Ad-CTRP9 or Ad-β-gal (n = 6 in each group) (lower). Ad-CTRP9 or Ad-β-gal (3.0×10^8 PFU total) was delivered intravenously via the tail vein 5 days before LPS injection (n = 6 in each group). (F) Cardiac levels of TNF-α and IL-6 in WT and AdipoR1-KO mice at 6 h after LPS injection. mRNA levels of TNF-α and IL-6 in the myocardium of WT and AdipoR1-KO mice receiving Ad-CTRP9 or Ad-β-gal were quantified by real-time PCR method and expressed relative to β-actin mRNA levels (n = 5 in each group). The results are presented as means ± the SEM.

sponses in various types of cells (26, 27). However, it has been reported that AMPK activation is unlikely to primarily participate in the salutary action of CTRP9 on adverse cardiac remodeling in mice after myocardial infarction (MI) (13), and cell culture experiments suggest that protein kinase A (PKA)-dependent inhibition of myocyte apoptosis is involved in CTRP9-mediated protection in post-MI remodeling (13). In this regard, our *in vitro* findings indicate that the anti-inflammatory effect of CTRP9 in cardiac myocytes is partly dependent on its ability to promote cAMP signaling. Moreover, CTRP9-KO mice had a lower level of myocardial cAMP after LPS injection compared to WT mice. Thus, it is conceivable that, in addition to AMPK, cAMP/PKA activation may be involved in the beneficial actions of CTRP9 on acute damage in the myocardium.

The current study provides the first *in vivo* evidence that AdipoR1 mediates the cardioprotective actions of CTRP9. CTRP9 supplementation had no protective effect on cardiac dysfunction in response to LPS in AdipoR1-KO mice. Furthermore, AdipoR1 was an essential mediator of CTRP9-induced suppression of myocardial inflammatory response to LPS *in vivo*. The *in vitro* data also showed that ablation of AdipoR1 reversed the inhibitory effect of CTRP9 on LPS-stimulated expression of inflammatory cytokines in cardiac myocytes. Moreover, our data showed that AdipoR1 mediates CTRP9-induced AMPK activation in both cultured cardiac myocytes and myocardium of mice. Therefore, it is plausible that CTRP9 reduces inflammatory response in cardiac myocytes through activation of AdipoR1-dependent AMPK. It has also been shown that CTRP9 promotes endothelial cell function and AMPK activation *in vitro* through an AdipoR1-dependent pathway (10). Moreover, we have shown that CTRP9 suppresses cardiomyocyte apoptosis *in vitro* through AdipoR1 (12). Accordantly, the present data indicated that CTRP9 deficiency causes increased apoptosis in the heart after ischemia-reperfusion. Collectively, these data suggest that CTRP9 improves inflammatory response and apoptosis in myocardium through its ability to activate AdipoR1-dependent AMPK signaling in its target cells, thereby leading to protection against acute cardiac injury.

In conclusion, we show that endogenous CTRP9 protects against acute cardiac damage in response to pathological stimuli by suppressing inflammatory reactions in cardiac myocytes. CTRP9 activates AMPK signaling cascades via a receptor-dependent pathway involving AdipoR1, and the activation of this signaling pathway attenuates expression of inflammatory cytokines such as TNF-α and IL-6. Notably, circulating CTRP9 levels are reduced in association with acute or chronic myocardial ischemia (12, 13). Thus, CTRP9 supplementation might be beneficial for the treatment or prevention of various heart diseases, including ischemic heart disease.

ACKNOWLEDGMENTS

We gratefully acknowledge Morris J. Birnbaum (University of Pennsylvania) for generously providing the dnAMPK-TG mice. We also acknowledge the technical assistance of Yoko Inoue.

This study was supported by Grant-in-Aid for Scientific Research and grants from Takeda Science Foundation and by a AstraZeneca Research and Development grant to N.O. R.S. was supported by a Grant-in-Aid for Scientific Research C, Banyu Life Science Foundation International, and Kanae Foundation.

REFERENCES

1. **Wolk R, Berger P, Lennon RJ, Brilakis ES, Somers VK.** 2003. Body mass index: a risk factor for unstable angina and myocardial infarction in patients with angiographically confirmed coronary artery disease. Circulation **108:** 2206–2211. http://dx.doi.org/10.1161/01.CIR.0000095270.85646.E8.
2. **Orlander PR, Goff DC, Morrissey M, Ramsey DJ, Wear ML, Labarthe DR, Nichaman MZ.** 1994. The relation of diabetes to the severity of acute myocardial infarction and post-myocardial infarction survival in Mexican-Americans and non-Hispanic whites. The Corpus Christi Heart Project. Diabetes **43:**897–902.
3. **Ouchi N, Parker JL, Lugus JJ, Walsh K.** 2011. Adipokines in inflammation and metabolic disease. Nat Rev Immunol **11:**85–97. http://dx.doi.org/10.1038/nri2921.
4. **Shibata R, Ohashi K, Murohara T, Ouchi N.** 2014. The potential of adipokines as therapeutic agents for cardiovascular disease. Cytokine Growth Factor Rev **25:**483–487. http://dx.doi.org/10.1016/j.cytogfr.2014.07.005.
5. **Ouchi N, Walsh K.** 2012. Cardiovascular and metabolic regulation by the adiponectin/C1q/tumor necrosis factor-related protein family of proteins. Circulation **125:**3066–3068. http://dx.doi.org/10.1161/circulationaha.112.114181.
6. **Wong GW, Krawczyk SA, Kitidis-Mitrokostas C, Ge G, Spooner E, Hug C, Gimeno R, Lodish HF.** 2009. Identification and characterization of CTRP9, a novel secreted glycoprotein, from adipose tissue that reduces serum glucose in mice and forms heterotrimers with adiponectin. FASEB J **23:**241–258. http://dx.doi.org/10.1096/fj.08-114991.
7. **Hwang YC, Woo Oh S, Park SW, Park CY.** 2014. Association of serum C1q/TNF-related protein-9 (CTRP9) concentration with visceral adiposity and metabolic syndrome in humans. Int J Obes **38:**1207–1212. http://dx.doi.org/10.1038/ijo.2013.242.
8. **Peterson JM, Wei Z, Seldin MM, Byerly MS, Aja S, Wong GW.** 2013. CTRP9 transgenic mice are protected from diet-induced obesity and metabolic dysfunction. Am J Physiol Regul Integr Comp Physiol **305:**R522–R533. http://dx.doi.org/10.1152/ajpregu.00110.2013.
9. **Wei Z, Lei X, Petersen PS, Aja S, Wong GW.** 2014. Targeted deletion of C1q/TNF-related protein 9 increases food intake, decreases insulin sensitivity, and promotes hepatic steatosis in mice. Am J Physiol Endocrinol Metab **306:**E779–E790. http://dx.doi.org/10.1152/ajpendo.00593.2013.
10. **Zheng Q, Yuan Y, Yi W, Lau WB, Wang Y, Wang X, Sun Y, Lopez BL, Christopher TA, Peterson JM, Wong GW, Yu S, Yi D, Ma XL.** 2011. C1q/TNF-related proteins, a family of novel adipokines, induce vascular relaxation through the adiponectin receptor-1/AMPK/eNOS/nitric oxide signaling pathway. Arterioscler Thromb Vasc Biol **31:**2616–2623. http://dx.doi.org/10.1161/atvbaha.111.231050.
11. **Uemura Y, Shibata R, Ohashi K, Enomoto T, Kambara T, Yamamoto T, Ogura Y, Yuasa D, Joki Y, Matsuo K, Miyabe M, Kataoka Y, Murohara T, Ouchi N.** 2013. Adipose-derived factor CTRP9 attenuates vascular smooth muscle cell proliferation and neointimal formation. FASEB J **27:**25–33. http://dx.doi.org/10.1096/fj.12-213744.
12. **Kambara T, Ohashi K, Shibata R, Ogura Y, Maruyama S, Enomoto T, Uemura Y, Shimizu Y, Yuasa D, Matsuo K, Miyabe M, Kataoka Y, Murohara T, Ouchi N.** 2012. CTRP9 protein protects against myocardial injury following ischemia-reperfusion through AMP-activated protein kinase (AMPK)-dependent mechanism. J Biol Chem **287:**18965–18973. http://dx.doi.org/10.1074/jbc.M112.357939.
13. **Sun Y, Yi W, Yuan Y, Lau WB, Yi D, Wang X, Wang Y, Su H, Wang X, Gao E, Koch WJ, Ma XL.** 2013. C1q/tumor necrosis factor-related protein-9, a novel adipocyte-derived cytokine, attenuates adverse remodeling in the ischemic mouse heart via protein kinase A activation. Circulation **128:**S113–S120. http://dx.doi.org/10.1161/CIRCUATIONAHA.112.000010.
14. **Ouchi N, Kobayashi H, Kihara S, Kumada M, Sato K, Inoue T, Funahashi T, Walsh K.** 2004. Adiponectin stimulates angiogenesis by promoting cross-talk between AMP-activated protein kinase and Akt signaling in endothelial cells. J Biol Chem **279:**1304–1309. http://dx.doi.org/10.1074/jbc.M310389200.
15. **Kobayashi H, Ouchi N, Kihara S, Walsh K, Kumada M, Abe Y, Funahashi T, Matsuzawa Y.** 2004. Selective suppression of endothelial cell apoptosis by the high molecular weight form of adiponectin. Circ Res **94:**e27–e31. http://dx.doi.org/10.1161/01.RES.0000119921.86460.37.
16. **Mu J, Brozinick JT, Jr, Valladares O, Bucan M, Birnbaum MJ.** 2001. A role for AMP-activated protein kinase in contraction- and hypoxia-

regulated glucose transport in skeletal muscle. Mol Cell **7:**1085–1094. http://dx.doi.org/10.1016/S1097-2765(01)00251-9.

17. **Valenzuela DM, Murphy AJ, Frendewey D, Gale NW, Economides AN, Auerbach W, Poueymirou WT, Adams NC, Rojas J, Yasenchak J, Chernomorsky R, Boucher M, Elsasser AL, Esau L, Zheng J, Griffiths JA, Wang X, Su H, Xue Y, Dominguez MG, Noguera I, Torres R, Macdonald LE, Stewart AF, DeChiara TM, Yancopoulos GD.** 2003. High-throughput engineering of the mouse genome coupled with high-resolution expression analysis. Nat Biotechnol **21:**652–659. http://dx.doi.org/10.1038/nbt822.
18. **Watanabe Y, Shibata R, Ouchi N, Kambara T, Ohashi K, Jie L, Inoue Y, Murohara T, Komori K.** 2014. Adiponectin ameliorates endotoxin-induced acute cardiac injury. Biomed Res Int **2014:**382035. http://dx.doi.org/10.1155/2014/382035.
19. **Shibata R, Sato K, Pimentel DR, Takemura Y, Kihara S, Ohashi K, Funahashi T, Ouchi N, Walsh K.** 2005. Adiponectin protects against myocardial ischemia-reperfusion injury through AMPK- and COX-2-dependent mechanisms. Nat Med **11:**1096–1103. http://dx.doi.org/10.1038/nm1295.
20. **Hayakawa S, Ohashi K, Shibata R, Kataoka Y, Miyabe M, Enomoto T, Joki Y, Shimizu Y, Kambara T, Uemura Y, Yuasa D, Ogawa H, Matsuo K, Hiramatsu-Ito M, van den Hoff MJ, Walsh K, Murohara T, Ouchi N.** 2015. Cardiac myocyte-derived follistatin-like 1 prevents renal injury in a subtotal nephrectomy model. J Am Soc Nephrol **26:**636–646. http://dx.doi.org/10.1681/ASN.2014020210.
21. **Frangogiannis NG, Smith CW, Entman ML.** 2002. The inflammatory response in myocardial infarction. Cardiovasc Res **53:**31–47. http://dx.doi.org/10.1016/S0008-6363(01)00434-5.
22. **Peng T, Lu X, Feng Q.** 2005. Pivotal role of gp91phox-containing NADH oxidase in lipopolysaccharide-induced tumor necrosis factor-alpha expression and myocardial depression. Circulation **111:**1637–1644. http://dx.doi.org/10.1161/01.CIR.0000160366.50210.E9.
23. **Hao E, Lang F, Chen Y, Zhang H, Cong X, Shen X, Su G.** 2013. Resveratrol alleviates endotoxin-induced myocardial toxicity via the Nrf2 transcription factor. PLoS One **8:**e69452. http://dx.doi.org/10.1371/journal.pone.0069452.
24. **Ogura Y, Ouchi N, Ohashi K, Shibata R, Kataoka Y, Kambara T, Kito T, Maruyama S, Yuasa D, Matsuo K, Enomoto T, Uemura Y, Miyabe M, Ishii M, Yamamoto T, Shimizu Y, Walsh K, Murohara T.** 2012. Therapeutic impact of follistatin-like 1 on myocardial ischemic injury in preclinical models. Circulation **126:**1728–1738. http://dx.doi.org/10.1161/circulationaha.112.115089.
25. **Gordon JW, Shaw JA, Kirshenbaum LA.** 2011. Multiple facets of NF-κB in the heart: to be or not to NF-κB. Circ Res **108:**1122–1132. http://dx.doi.org/10.1161/circresaha.110.226928.
26. **O'Neill LA, Hardie DG.** 2013. Metabolism of inflammation limited by AMPK and pseudo-starvation. Nature **493:**346–355. http://dx.doi.org/10.1038/nature11862.
27. **Fisslthaler B, Fleming I.** 2009. Activation and signaling by the AMP-activated protein kinase in endothelial cells. Circ Res **105:**114–127. http://dx.doi.org/10.1161/circresaha.109.201590.
28. **Parker-Duffen JL, Nakamura K, Silver M, Zuriaga MA, MacLauchlan S, Aprahamian TR, Walsh K.** 2014. Divergent roles for adiponectin receptor 1 (AdipoR1) and AdipoR2 in mediating revascularization and metabolic dysfunction in vivo. J Biol Chem **289:**16200–16213. http://dx.doi.org/10.1074/jbc.M114.548115.